Scandinavian Cardiovascular Journal

ISSN: (Print) (Online) Journal homepage: https://www.tandfonline.com/loi/icdv20

Remote ischemic preconditioning and hypoxia-induced biomarkers in acute myocardial infarction: study on a porcine model

Tuomas Anttila, Johanna Herajärvi, Henna Laaksonen, Caius Mustonen, Hannu-Pekka Honkanen, Elitsa Y. Dimova, Jarkko Piuhola, Peppi Koivunen, Tatu Juvonen & Vesa Anttila

To cite this article: Tuomas Anttila, Johanna Herajärvi, Henna Laaksonen, Caius Mustonen, Hannu-Pekka Honkanen, Elitsa Y. Dimova, Jarkko Piuhola, Peppi Koivunen, Tatu Juvonen & Vesa Anttila (2023) Remote ischemic preconditioning and hypoxia-induced biomarkers in acute myocardial infarction: study on a porcine model, Scandinavian Cardiovascular Journal, 57:1, 2251730, DOI: 10.1080/14017431.2023.2251730

To link to this article: https://doi.org/10.1080/14017431.2023.2251730

Published online: 29 Aug 2023.

SCANDINAVIAN CARDIOVASCULAR JOURNAL
2023, VOL. 57, NO. 1, 2251730
https://doi.org/10.1080/14017431.2023.2251730

Taylor & Francis
Taylor & Francis Group

RESEARCH ARTICLE

OPEN ACCESS Check for updates

Remote ischemic preconditioning and hypoxia-induced biomarkers in acute myocardial infarction: study on a porcine model

Tuomas Anttila[a], Johanna Herajärvi[a], Henna Laaksonen[a], Caius Mustonen[a], Hannu-Pekka Honkanen[a], Elitsa Y. Dimova[b], Jarkko Piuhola[c], Peppi Koivunen[b], Tatu Juvonen[a,d] and Vesa Anttila[e]

[a]Research Unit of Surgery, Anesthesia and Intensive Care, Department of Surgery, Oulu University Hospital and Medical Research Center Oulu, University of Oulu, Oulu, Finland; [b]Faculty of Biochemistry and Molecular Medicine, Biocenter Oulu, Oulu Center for Cell-Matrix Research, University of Oulu, Oulu, Finland; [c]Department of Cardiology, Oulu University Hospital and Medical Research Center Oulu, University of Oulu, Oulu, Finland; [d]Department of Cardiac Surgery, Heart and Lung Center, Helsinki University Hospital, University of Helsinki, Helsinki, Finland; [e]Heart Center, Turku University Hospital, University of Turku, Turku, Finland

ABSTRACT

Objectives. Remote ischemic preconditioning (RIPC) mitigates acute myocardial infarction (AMI). We hypothesized that RIPC reduces the size and severity of AMI and explored molecular mechanisms behind this phenomenon. *Design.* In two series of experiments, piglets underwent 60 min of the circumflex coronary artery occlusion, resulting in AMI. Piglets were randomly assigned into the RIPC groups ($n = 7 + 7$) and the control groups ($n = 7 + 7$). The RIPC groups underwent four 5-min hind limb ischemia-reperfusion cycles before AMI. In series I, the protective efficacy of RIPC was investigated by using biomarkers and echocardiography with a follow-up of 24 h. In series II, the heart of each piglet was harvested for TTC-staining to measure infarct size. Muscle biopsies were collected from the hind limb to explore molecular mechanisms of RIPC using qPCR and Western blot analysis. *Results.* The levels of CK-MBm ($p = 0.032$) and TnI ($p = 0.007$) were lower in the RIPC group. Left ventricular ejection fraction in the RIPC group was greater at the end of the follow-up. The myocardial infarct size in the RIPC group was smaller ($p = 0.033$). Western blot indicated HIF1α stabilization in the skeletal muscle of the RIPC group. PCR analyses showed upregulation of the HIF target mRNAs for glucose transporter (GLUT1), glucose transporter 4 (GLUT4), phosphofructokinase 1 (PFK1), glyceraldehyde 3-phosphate dehydrogenase (GAPDH), enolase 1 (ENO1), lactate dehydrogenase (LDHA) and endothelial nitric oxidate synthase (eNOS). *Conclusions.* Biochemical, physiologic, and histologic evidence confirms that RIPC decreases the size of AMI. The HIF pathway is likely involved in the mechanism of the RIPC.

ARTICLE HISTORY
Received 11 May 2023
Revised 19 July 2023
Accepted 18 August 2023

KEYWORDS
Remote ischemic preconditioning; acute myocardial infarction; hypoxia-inducible factor; cardiac protection; mRNA; planimetry

Introduction

Despite the success of revascularization therapy, acute myocardial infarction (AMI) remains one of the leading causes of morbidity and mortality worldwide [1]. Occluded coronary artery and subsequent inadequate blood flow lead to lack of oxygen, ischemia, and the death of cardiomyocytes resulting in an acute myocardial infarction (AMI). The loss of a large number of cardiomyocytes impairs cardiac function.

Ischemic preconditioning has been introduced as a strategy to mitigate ischemic damage [2]. In remote ischemic preconditioning (RIPC), short periods of non-lethal ischemia followed by reperfusion of non-target tissue prepare remote tissues and organs to resist a subsequent more severe ischemia-reperfusion injury [3]. Animal and human studies suggest that RIPC reduces endothelial dysfunction and myocardial hypoxic damage after coronary artery occlusion, and RIPC is reported to improve even long-term cardiovascular outcomes [4–8]. Transmitting mechanisms of cardioprotective stimuli from the remote tissue to the myocardium remains still unclear, but neurogenic, hormonal, and systemic factors have been proposed to play a role [9]. Bloodborne circulatory factors have been suggested to be responsible for transferable protective action in the target organ [10–13]. Some previous studies indicate that hypoxia-inducible factor (HIF) may play a role in the preconditioning process [14–16].

In the present study, we explored whether RIPC mitigates myocardial damage in a porcine model of AMI and examined possible molecular mechanisms responsible for cardioprotection, particularly the potential role of HIF.

Materials and methods

Preoperative care and anaesthesia

All animals received humane care in accordance with the European Union (EU directive on the protection of animals used for scientific purposes 2010/63/EU) and the Finnish legislation on the protection of animals used for scientific

CONTACT Vesa Anttila vesa.anttila@tyks.fi Heart Center, Turku University Hospital, Turku University, P.O. Box 52, Turku 20521, Finland

purposes (FINLEX 497/2013). The study protocol was approved by the Finnish National Animal Experiment Board (ESAVI/2581/04.10.07/2014). The piglets were housed in the same cage with a mellow environment at least seven days before the experiments. The social nature of the animals was taken into consideration preoperatively. The Research Animal Care and Use Committee of Oulu University, Oulu, Finland approved the experimental set-ups and protocols.

The animals were sedated by an intramuscular injection of ketamine (350 mg), midazolam (45 mg), and medetomidine (1.5 mg). Intravenous catheters were inserted into a vein in both ears. During anesthesia induction the piglets received intravenous thiopental (25–125 µg) and fentanyl (0.5 mg), and a prophylactic antibiotic (cefuroxime 1.5 g). A very low dose thiopental was chosen, because of previous reports on propofol possibly affecting RIPC. A 6.0 mm cuffed endotracheal tube was used for intubation, and the respirator was set to a ventilation of 55/45% oxygen-air-ratio. Continuous anesthesia was achieved by combining an intravenous anesthetic consisting of fentanyl (0.025 mg/kg/h) and ketamine (15 mg/kg/h) as well as inhaled sevoflurane (1.0%). The animals received a single dose of rocuronium (0.05 mg/kg) before the onset of surgical procedures to allow surgical relaxation.

Experimental setting

The study protocol is presented in Figure 2 Figure 1. In two series of experiments, a total of 28 juvenile female piglets (8–10 weeks of age, weighing 23–27 kg) from a native stock were studied. In both series, the piglets were randomized either to the RIPC ($n = 7 + 7$) or the control groups ($n = 7 + 7$) by picking up a sealed envelope before the operation. In Series I, we studied whether RIPC is cardioprotective in AMI and measured serum cardiac biomarker levels as well as ventricular ejection fractions by transthoracic echocardiography serially with a total follow-up time of 24 h. In series II, the size of AMI was quantified and the molecular mechanisms of RIPC as well as hypoxia-related biomarkers were explored. In both series, the RIPC and AMI protocols were the same. In series II, a shorter follow-up time of 4 h was used to determine the level of hypoxia-induced biomarkers from the harvested tissues during the acute phase to explore molecular mechanisms of RIPC.

After the induction of anesthesia, a pulmonary artery thermodilution catheter (CritiCath; Ohmeda GmbH, Erlangen, Germany) was inserted surgically through the right femoral vein. The thermodilution catheter allowed invasive hemodynamic monitoring and blood sampling. An arterial cannula was inserted into the right femoral artery to allow continuous blood pressure measurements and blood sample collections. A urine catheter was placed to measure urine volume during the operation and to assess fluid balance. Rectal temperature was measured continuously throughout the experiment.

Remote ischemic preconditioning

Before the coronary artery occlusion, the RIPC group underwent four cycles of 5-min ischemia-reperfusion cycles (Figure 2). The 9 cm wide blood pressure cuff was placed around the left hind limb, and the cuff was inflated to 350 mmHg for 5 min, followed by a 5-min deflation. RIPC consisted of four inflation-deflation cycles, and the total duration of RIPC was 40 min. The control group received sham treatment with the blood pressure cuff set to a pressure of 0 mmHg.

Acute myocardial ischemia

After the exposure of the heart through a left anterolateral thoracotomy in the fourth intercostal space, the bifurcation of the left anterior descending (LAD) and the left circumflex (LCX) coronary arteries was identified. After preconditioning or sham treatment the LCX was occluded proximally to the bifurcation by using a removable silicone vascular loop (Surg-I-Loop, Scanlan, St. Paul, MN, USA). Intravenous lidocain (2 mg/kg) was given to prevent cardiac arrhythmias. The occlusion of the LCX blood flow was confirmed by using a 5 mm transit time flow meter sensor (CardioMed-2000, Medistim, Norway). The vascular loop was removed after 60 min of occlusion to allow reperfusion. Papaverine (20 mg) was topically applied over the artery to prevent the artery spasm. Finally, surgical incisions were closed. The piglets were kept under anesthesia until the end of the experiment and euthanised before the tissue harvest.

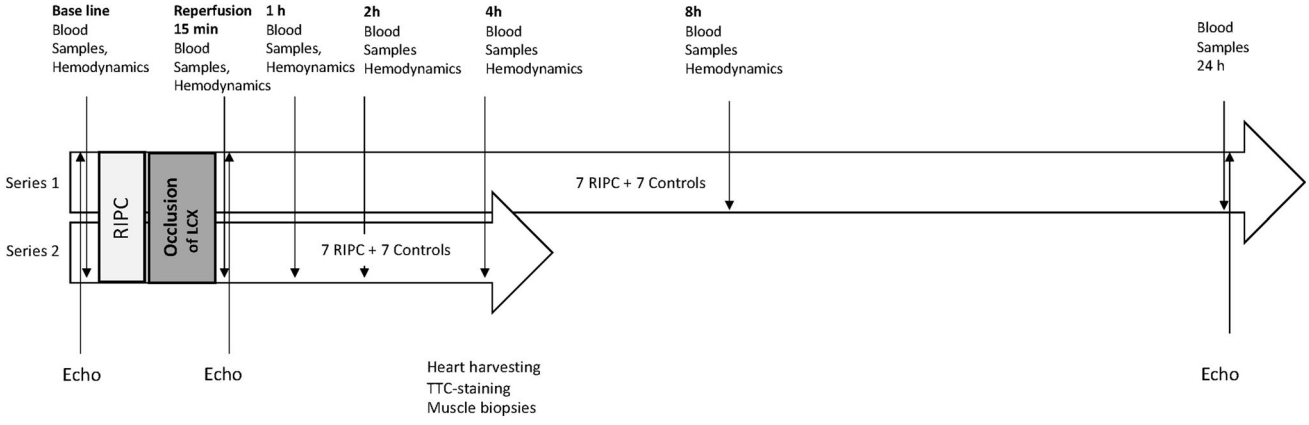

Figure 1. A graphical abstract of the chosen study protocol. The figure shows the number of pigs in each series, the time points used for sampling, biopsies, echocardiography and tissue collection, as well as the timing of RIPC and left coronary artery occlusion.

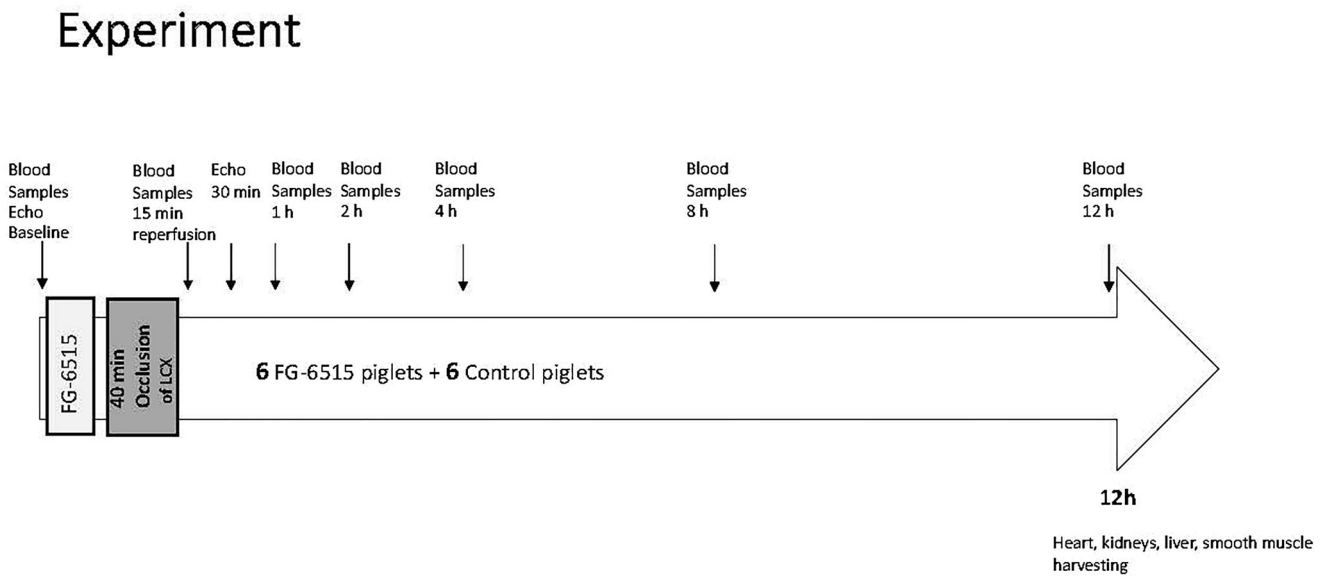

Figure 2. Study protocol. A graphical abstract of the chosen study protocol. Decipted are the number of pigs in each series and subgroup. The image shows time-points used for sampling, biopsies, echocardiography, and tissue harvest as well as the timing of RIPC and occlusion of the left circumflex artery.

Hemodynamic monitoring and blood sampling

Arterial blood pressure was monitored continuously with a right femoral artery cannula. Urine secretion was measured to assess fluid balance. Baseline venous blood sampling was done before the surgical operation, and post-RIPC sampling immediately after the last RIPC cycle before the operation. Post-infarct blood samples were drawn at 15 min, 1, 2, 4, 8, and 24 h after the initiation of the reperfusion in both series (Figure 2). At these time points blood gases, lactate, electrolytes, glucose, hemoglobin, hematocrit, and ionized calcium levels (iStat Analyzer, iStat Corporation, East Windsor, NJ, USA) as well as levels of troponin I (TnI) and Creatine Kinase-MBm (CK-MBm) were measured (electrochemiluminescence immunoassay, NordLab, Oulu, Finland).

Echocardiography

Transthoracic echocardiography was performed by using an Acuson Seqouia 512 echo system with a 3.5 MHz transducer (Siemens; Munich, Germany) at baseline, post-infarct (30 min after reperfusion) and at 24 h after instituting reflow (in the series I only, Figure 2). A single experienced cardiologist (JP) blinded to the treatment group performed the echocardiographic examinations. Systolic function was evaluated by calculation of left ventricular ejection fraction. Ejection fraction (EF) was measured by single-plane area length and calculated according to the formula: EF (%) = [(0.85 $LVAD^2$/LVLD) − [0.85 $LVAS^2$/LVLS)]/(0.85 $LVAD^2$/LVLD) × 100, where LVAD = left ventricular area in end-diastole; LVAS = left ventricular area in end-systole; LVLD = left ventricular long-axis length in end-diastole; and LVLS = left ventricular long-axis length in end-systole. This method has been previously used in animal studies [8].

Evaluation of the infarct size

At the end of the reperfusion period, the LCX coronary artery was re-occluded at the same location and 100 ml of 2% Evans Blue dye was injected to define the area at risk (AAR) (unstained) and perfused myocardium (stained blue). The hearts were excised and frozen immediately at −70 °C. A semi-frozen heart was sectioned into 4–5 equal slices from the apex to the base of the heart and incubated with 1% triphenyltetrazolium chloride (TTC, Sigma Aldrich, St Louis, MO, USA) for 30 min at 37 °C to discriminate the infarcted tissue from the viable myocardium. The slices were photographed with a digital camera (Nikon D7100) from both sides. Left ventricle area (LV), area at risk (AAR), and infarct area (IA) were measured by a digital planimetry (Adobe Photoshop CS5, Adobe, San Jose, CA, USA) on both sides of each slice, and the arithmetic mean area was calculated. The IA/LV-, AAR/LV, and IA/AAR-ratios were calculated by a single experienced researcher (ED) blinded for the study protocol.

Quantitative real-time PCR analyses for hypoxia-induced biomarkers

After the experiment, skeletal muscle biopsies from the porcine hind limbs were harvested and snap-frozen in liquid nitrogen and stored at −70 °C. Muscle tissue was homogenized using a tissue homogenizer (TissueLyser LT, Qiagen, Hilden, Germany), and RNA was isolated using TriPure isolation reagent (Roche, Basel, Switzerland) and purified using EZNA total RNA kit (Omega Bio-Tek, Norcross, GA, USA) according to the manufacturer's instructions. Two hundred nanograms of total RNA was used for cDNA synthesis with iScript™ cDNA synthesis Kit (Bio-Rad Laboratories, Hercules, CA, USA). Quantitative real-time PCR was performed in a CFX96 Real-Time System (Bio-Rad Laboratories, Hercules, CA, USA) by using an iTaq™ Universal SYBR® green PCR Supermix (Bio-Rad Laboratories, Hercules, CA, USA). Sequences of the primers used in the study are listed in Table 1. Porcine 18S rRNA

(RN18S) was used as internal control to normalize the variability in expression levels. Analysis was done for HIF1A, HIF2A (EPAS), Glucose transporter 1 (GLUT1), GLUT4, Phosphofructokinease-1 (PFK1), Glyceraldehyde-3-Phosphate Dehydrogenase (GADPH), Enolase 1 (ENO1), Lactate dehydrogenease (LDHA) and endothelial nitric oxide synthase (eNOS/NOS3).

Western blot

Skeletal muscle biopsies from porcine hind limbs were snap-frozen in liquid nitrogen and stored at −70 °C. Muscle tissue was homogenized using a tissue homogenizer (TissueLyser LT, Qiagen, Hilden, Germany). Total protein was extracted with buffer containing 3 M urea, 75 mM NaCl, 25 mM Tris-HCl, 0.25% NP-40, and a complete protease inhibitor (Roche) was used. The protein concentrations were estimated by the Bradford method (Bio-Rad protein assay). Proteins (100 µg per sample) were separated by electrophoresis on 7.5% polyacrylamide gels and transferred to nitrocellulose membranes. Membranes were incubated with anti-HIF1 (1:1000) (Novus Biologicals, Littleton, CO, USA), or mouse anti-alpha tubulin (1:5000) (Sigma Aldrich, St Louis, MO, USA) antibodies overnight at 4 °C. Appropriate secondary antibodies were used in 1:5000 dilutions. The enhanced chemiluminescence kit (Amersham Pharmacia Biotech, Little Chalfont, UK) was used for the detection of immunoreactive bands.

Table 1. Sequence of primers used for quantitative polymerase chain reaction analysis.

Gene	Forward (5′-3′)	Reverse (5′-3′)
HIF1A	TGCTGGTGATTTGGATATTGAAGA	ACAAAACCATCCAAGGCTTTCA
EPAS1 (HIF2A)	TTGCCGTAGTGACCCAGGAT	CCTGTTAGCTCCACCTGTGT
GLUT1	CCAAGAGCGTGCTGAAGAAG	GTGACCTTCTTCTCCCGCAT
GLUT4	CCACTACTCCTGGGCATCAC	GTCAGGCGCTTCAGACTCTT
PFK1	GCTACGTCAAGGACCTGGTG	ATGCCCATCTTGCTGCTCAG
GAPDH	AGCTCATTTCCTGGTACGACAA	AGGGGCTCTTACTCCTTGGA
ENO1	TGGGGAAAGGTGTCTCAAAGG	TGCTCCACGACGTTCAGTTT
LDHA	GAAGTGCACTCCCGATTCCT	AACAGCACCAACCCCAACAA
NOS3 (eNOS)	GGAAGCTGCAGGTGTTCGAT	CGGTTGGTGGCGTACTTGAT
RN18S	GGCTACCACATCCAAGGAAG	TCCAATGGATCCTCGCGGAA

The same sequence was used for all the analyses.

Statistical analyses

Continuous variables are expressed as medians with 25th–75th percentiles. The repeated measurements were analysed using a linear mixed model with animals fitted as random, and the best covariance pattern was chosen according to Akaike's information criteria. Complete independence was assumed across animals (by random statement). Reported *p*-values are as follows: *p* between groups (p_g) indicates a level of difference between groups, *p* time * group (p_{t*g}) indicates behaviour between groups over time.

At single timepoints, the distribution of the continuous data was evaluated by Kolmogorov–Smirnov test. The Student's *t*-test was employed, if the data were normally distributed. Otherwise, the Mann–Whitney *U* test was chosen. A *p*-value <0.05 was considered statistically significant. The statistical analyses were conducted by using SPSS (IBM® Corporation, Armonk, NY, USA, version 24.0.0).

Results

Cardiac findings

Digital planimetry showed smaller infarct areas per left ventricular area (as a percentage) in the RIPC group compared to the control group (22.0 ± 11.0 *vs.* 33.3 ± 4.9, $p = 0.03$) (Figure 3).

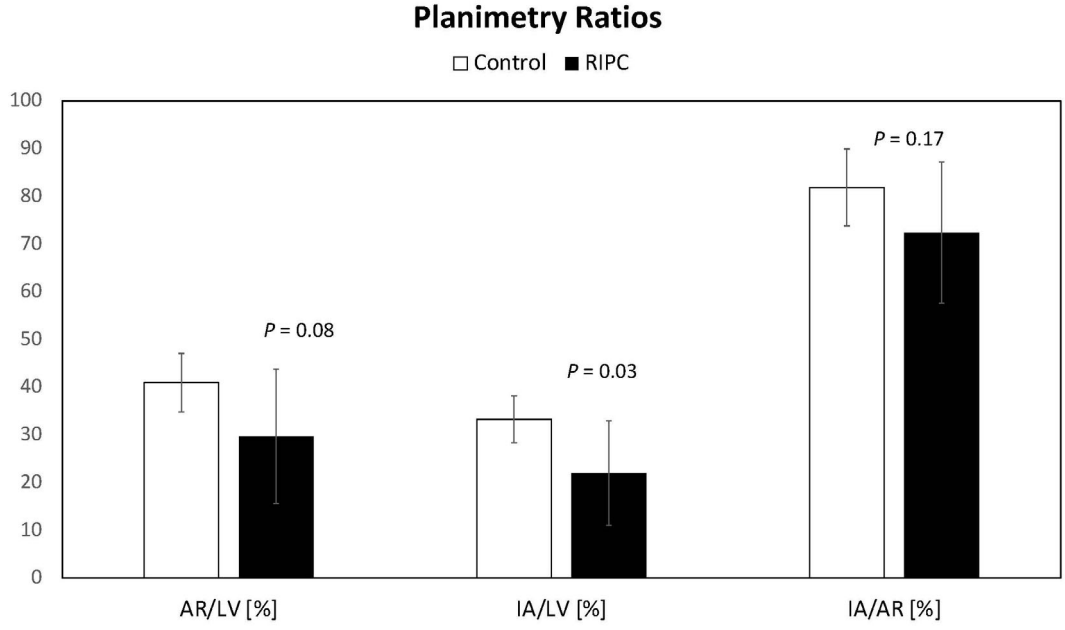

Figure 3. Planimetry ratios. Using digital planimetry the arithmetic areas of area at risk (AR), infarct area (IA) and left ventricle area (LV) were calculated. Independent samples *t*-test was used to compare area at risk (AR) per area of the left ventricle (LV) ($p = 0.08$), infarct area (IA) per left ventricle (LV) ($p = 0.03$), and infarct area (IA) per area at risk (AR) ($p = 0.17$). The number of pigs in each group is 7.

Table 2. Hemodynamic data.

	Baseline	Post-RIPC	15 min	1 h	2 h	4 h	p_g	$p_t{}^*{}_g$
Heart rate (bpm)							<0.01	0.66
RIPC	87 (78–115)	105 (80–113)*	113 (91–121)**	112 (102–124)	111 (105–129)*	118 (107–133)*		
Control	103 (91–120)	107 (102–126)	127 (120–146)	125 (117–138)	133 (110–146)	131 (120–146)		
Mean arterial pressure, mmHg							0.31	0.65
RIPC	95 (85–103)	79 (74–94)	68 (63–78)	70 (62–78)	67 (64–71)	65 (62–69)		
Control	99 (84–111)	83 (76–96)	70 (65–79)	75 (70–81)	74 (68–80)	64 (62–71)		
Pulmonary artery pressure, mmHg							0.11/<0.01	0.94/0.68
RIPC	20 (19–22)/ 11 (10–12)	20 (19–22)/ 10 (9–11)	18 (17–21)/ 11 (10–14)	21 (20–23)/ 12 (11–14)	21 (19–24)/ 12 (11–14)*	22 (20–26)/ 12(12–16)		
Control	20 (19–24)/ 12 (11–14)	20 (19–25)/ 12 (9–13)	20 (19–24)/ 13 (12–14)	22 (20–27)/ 13 (12–15)	23 (20–26)/ 14 (11–14)	25 (22–29)/ 14 13–18)		
Cardiac Output, mL*min^{-1}							0.83	<0.01
RIPC	2.67 (2.29–3.12)	2.78 (2.45–2.90)	2.23 (1.87–2.83)	2.58 (2.24–2.74)	2.40 (2.55–2.70)*	2.00 (1.58–2.75)		
Control	3.07 (2.42–3.40)	2.58 (2.25–3.54)	2.30 (2.12–2.71)	2.28 (1.97–2.71)	1.97 (1.49–2.53)	2.02 (1.38–2.33)		
Central venous pressure, mmHg							0.71	0.42
RIPC	4 (3–5)	4 (3–4)	4 (3–6)	4 (3–4)	3 (2–4)	4 (2–5)		
Control	4 (3–5)	3 (3–5)	4 (3–5)	4 (2–4)	4 (2–4)	4 (3–5)		
Blood temperature, °C							0.76	0.62
RIPC	37.9 (37.5–38.5)	38.2 (37.4–38.6)	38.2 (37.2–38.7)	37.7 (36.8–38.6)	37.2 (36.7–38.2)	37.3 (36.9–38.1)		
Control	38.2 (37.5–38.5)	38.2(37.6–38.7)	38.3 (37.1–38.9)	37.8 (37.0–38.7)	37.5 (37.1–38.4)	37.6 (36.8–39.0)		

General linear model. *N* (RIPC) = 14, *n* (control) = 14. Values are shown as medians and 25th and 75th percentiles.
*$p < 0.05$, **$p<0.01$ at a single timepoint. *p* Between the groups (p_g) indicates a level of difference between the groups and p_{g*t} indicates the difference between groups over time.

Table 3. Metabolic data.

	Baseline	Post-RIPC	15 min	1 h	2 h	4 h	p_g	$p_t{}^*{}_g$
Ph							0.70	0.11
RIPC	7.43 (7.39–7.47)	7.43 (7.39–7.48)	7.42 (7.38–7.47)	7.45 (7.41–7.47)	7.46 (7.43–7.48)	7.45 (7.43–7.48)		
Control	7.46 (7.41–7.49)	7.47 (7.42–7.49)	7.44 (7.41–7.48)	7.45 (7.43–7.47)	7.44 (7.42–7.47)	7.42 (7.40–7.48)		
Venous pCO_2, kPa							0.76	0.20
RIPC	6.28 (6.10–6.64)	6.28 (5.97–6.49)	6.40 (6.18–6.82)	6.23 (5.97–6.62)	6.13 (5.95–6.64)	6.29 (5.97–6.64)		
Control	6.28 (5.97–6.49)	6.10 (5.90–6.29)	6.30 (5.86–6.68)	6.28 (6.01–6.63)	6.39 (6.19–6.97)	6.29 (5.87–6.97)		
Venous pO_2, kPa							0.86	0.02
RIPC	5.20 (5.00–5.80)	5.20 (5.05–5.50)	4.90 (4.60–5.10)	5.10 (4.75–5.50)	5.20 (4.65–5.40)	4.70 (4.25–5.45)		
Control	5.30 (5.01–5.95)	5.30 (5.05–5.90)	5.00 (4.60–5.90)	5.20 (4.55–5.50)	4.80 (4.25–5.45)	4.50 (4.25–4.95)		
Hemoglobin, g/L							0.01	0.27
RIPC	78 (74–90)*	82 (77–92)*	82 (77–88)**	92 (80–95)**	95 (87–99)*	99 (90–107)*		
Control	94 (82–102)	95 (87–105)	95 (89–104)	105 (91–109)	109 (95–118)	112 (98–121)		
Hematocrit, %							0.03	0.30
RIPC	23.0 (22.0–26.0)*	25.0 (22.5–27.0)	25.0 (22.5–26.0)*	27.0 (24.0–28.0)*	28.0 (25.5–29.5)*	29.0 (26.5–31.0)		
Control	28.0 (23.5–30.0)	28.0 (25.5–30.0)	28.0 (25.5–30.0)	31.0 (26.0–31.5)	32.0 (28.0–33.0)	32.0 (27.5–35.5)		
Venous lactate, mmol/L							0.96	0.30
RIPC	0.89 (0.72–1.28)	0.95 (0.71–1.29)	1.01 (0.69–1.29)	0.71 (0.52–0.98)	0.65 (0.51–0.76)	0.54 (0.46–0.66)		
Control	0.82 (0.71–0.99)	0.83 (0.69–0.95)	0.97 (0.71–1.25)	0.76 (0.56–0.98)	0.69 (0.52–0.90)	0.60 (0.54–0.85)		
Venous glucose, mmol/L							0.91	0.40
RIPC	5.8 (4.3–6.9)	5.6 (4.3–6.4)	5.2 (5.0–6.8)	5.6 (4.5–6.7)	4.9 (3.6–5.9)	3.6 (2.7–4.9)		
Control	6.1 (5.7–6.9)	6.1 (5.1–6.7)	6.2 (5.0–6.7)	5.6 (4.7–6.7)	4.1 (2.9–5.7)	3.8 (3.2–4.8)		

General linear model. *N* (RIPC) = 14, *n* (control) = 14. Values are shown as medians and 25th and 75th percentiles.
*$p < 0.05$, **$p < 0.01$ at a single timepoint. *p* Between the groups (p_g) indicates a level of difference between the groups and p_{g*t} indicates the difference between groups over time.

Groups did not differ at baseline in hemodynamic measurements. Heart rate was lower after AMI in the RIPC group. Cardiac output was higher at 2 h after AMI in RIPC group (Table 2). Hematocrit was lower at baseline, 15 min, 1 h, and 2 h after AMI in the RIPC group (Table 3). The TnI levels were significantly lower in the RIPC group at all post-infarct timepoints compared to the controls. The CK-MBm levels in the RIPC group were significantly lower at 15 min, 2 h, and 4 h after the infarction (Table 4).

The echocardiographic baseline EF did not differ between the RIPC and the control groups. The post-infarct EF values were better in the RIPC group [52 (43–58) *vs.* 44 (42–52)%, $p_g = 0.01$]. After a 24-h follow-up, the RIPC group had greater EF compared to the control group [51 (46–58) *vs.* 42 (37–50)%, $p_g = 0.01$]. Furthermore, the decrease in EF values from the baseline to the post-infarct values [9 (4–18) *vs.* 22 (16–26)%, $p_g = 0.001$] and to the 24-h evaluation was smaller in the RIPC group than in the controls [12 (5–15) *vs.* 24 (18–29)%, $p_g = 0.01$] (Figure 4).

Molecular analyses of the hypoxia-induced biomarkers

Western blotting of skeletal muscle biopsies from the hind limbs was performed to assess HIF1α stabilization. Stabilization of HIF1α was detected in the RIPC group but not in the controls (Figure 5). The mRNA levels of the HIF targets GLUT1, GLUT4, GAPDH, ENO1, and eNOS in quantitative real-time PCR analyses were significantly higher in the RIPC group compared to the controls (Figure 6). The difference in HIF2A, PFK1, and LDHA mRNA levels did

Table 4. Cardiac markers.

	Baseline	Post-RIPC	15 min	1 h	2 h	4 h	p_g	$p_t{}^*{}_g$
Creatinine kinease-MBm							0.03	0.06
RIPC	2.60 (2.05–4.01)	2.76 (2.06–4.6)	13.56 (7.78–24.8)*	43.4 (16.24–62.19)	56.8 (23.09–73.91)*	46.75 (25.11–61.78)*		
Control	3.09 (2.58–3.67)	3.10 (2.61–4.22)	26.30 (21.83–52.30)	67.58 (47.37–117.32)	74.04 (53.87–147.77)	71.88 (49.01–142.77)		
Troponin I							<0.01	<0.01
RIPC	0.07 (0.03–0,11)	0.10 (0.04–0.14)	14.23 (5.20–45.49)*	113.53 (50.36–184.69)*	154.94 (74.63–204.72)*	145.23 (63.51–201.33)**		
Control	0.14 (0.08–0.22)	0.19 (0.10–0.24)	58.48 (20.64–118.19)	267.53 (106.69–311.85)	298.73 (166.52–348.66)	304.27 (205.84–374.19)		

General linear model. The levels of creatine kinease-MBm and troponin I at different timepoints are shown. *N* (RIPC) = 14, *n* (control) = 14. Values are shown as medians and 25th and 75th percentiles.
$^*p < 0.05$, $^{**}p < 0.01$ at a single timepoint. *p* Between the groups (p_g) indicates a level of difference between the groups and p_{g^*t} indicates the difference between groups over time.

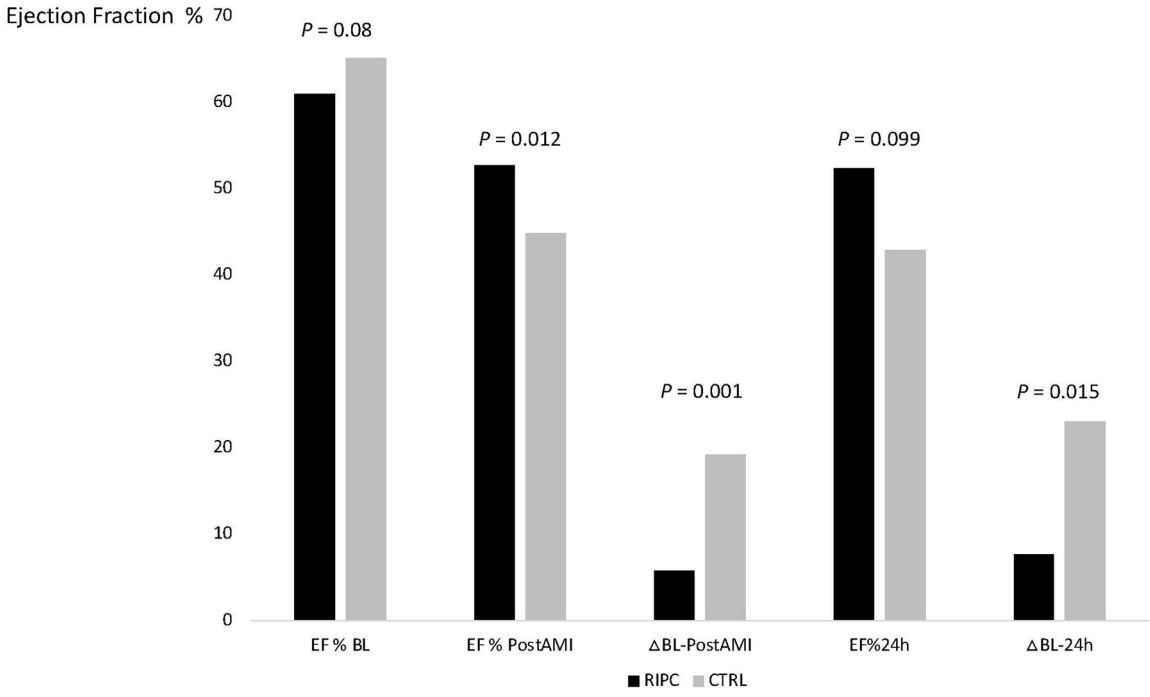

Figure 4. A bar graph showing the median (and 25th and 75th percentiles) of left ventricle ejection fractions at baseline (EF % BL), post-infarction (EF % PostAMI), and at 24 h after instituting reflow to the left circumflex artery (EF % 24 h). The decrease in EF values from the baseline to the post-infarct values (ΔBL-PostAMI) and to the 24-h evaluation (ΔBL-24 h) are also shown. Independent samples *t*-test was used and the *p*-values: EF % BL $p = 0.08$; EF % PostAMI $p = 0.01$; ΔBL-PostAMI $p = 0.001$; EF % 24 h $p = 0.01$; ΔBL-24 h $p = 0.01$. RIPC: remote ischemic preconditioning, *n* (RIPC) = 14, *n* (control) = 14 at the baseline and post-infarction timepoints, and *n* (RIPC) = 7, *n* (control) = 7 at the 24-h timepoint.

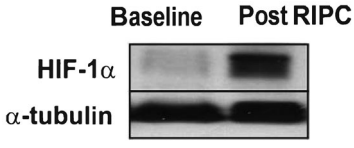

Figure 5. An image showing the stabilization of HIF1α after RIPC using the Western Blot method.

not reach statistical significance, but the values tended to be higher in the RIPC group compared to the controls (*p*-values: 0.10, 0.07, and 0.07, respectively) (Figure 6).

Discussion

The present porcine study shows that RIPC reduces the infarct size and helps to preserve cardiac function after acute myocardial infarction. Physiological, biochemical, and histological data collected in this study suggest that RIPC protects the myocardium, and the cardioprotective role of RIPC is mediated, at least in part, through HIF signaling pathways.

Infarct size quantification by digital planimetry showed reduced size infarct size after RIPC. Lower circulating levels of TnI and CK-MBm in the RIPC group emphasized this finding. Furthermore, greater left ventricular ejection fractions measured by echocardiography showed that in the RIPC group cardiac function was preserved better after the myocardial infarction than in the control group. Hemodynamic data indicated lower heart rates and pulmonary diastolic pressures as well as higher cardiac outputs in the RIPC group compared to the controls. These findings suggest that RIPC is cardioprotective, at least when cardiac ischemia occurs shortly after RIPC.

It has been suggested that the remote protection offered by RIPC is mediated by humoral factors, neuronal stimulus, and systemic inflammatory response [9]. In cardiac protection, humoral factors seem to play a greater role since even a denervated heart seems to benefit from RIPC [17]. The

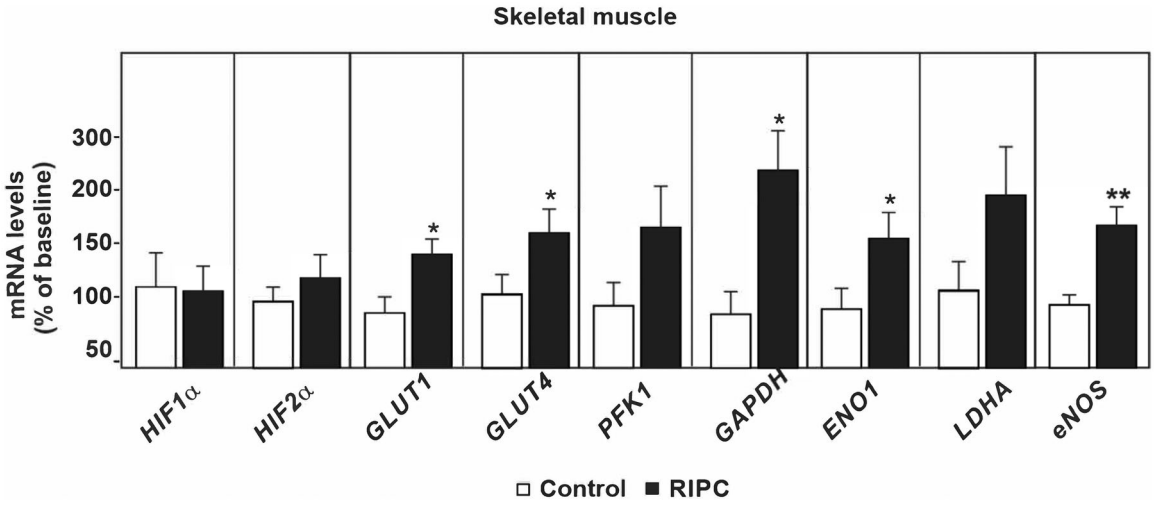

Figure 6. QPCR analysed mRNA levels from skeletal muscle biopsies shown in a bar graph. *N* (RIPC) = 7, *n* (control) = 7. *$p < 0.05$, **$p < 0.01$ in each analysis. The values shown are the means and standard error of the mean. Independent samples *t*-test was used.

precise mechanism by which RIPC protects the heart has remained elusive, and so far various substances, such as GLP-1 [18], specific amino acids [19], Janus kinase (JAK)-signal transducer and activator of the transcription (STAT)-activating cytokines [20] as well as HIF1α [16] have been proposed have a role in RIPC signalling. Recent studies have shown that small, anuclear, bilayered lipid membrane particles, known as extracellular vesicles (EVs), are drivers of signal transduction in cardioprotective RIPC. These EVs could potentially also be used as a drug delivery mechanism in the treatment of heart diseases [21]. Previous small animal studies have established that inhibiting HIF1α neutralizes the effects of RIPC [14]. RIPC also seems to regulate HIF1α levels [15, 22]. A study in mice showed that HIF1α activates gene transcription and is required for cardiac protection of RIPC [16].

HIF upregulates genes including, but not limited to erythropoetin, vasoendothelial growth factor, and glycolytic factors [23]. Our study shows through Western blotting that HIF1α was stabilized in the hind limb of pigs predisposed to RIPC. Interestingly our study demonstrates that GLUT1, GLUT4, GADPH, and eNOS levels were significantly higher in the RIPC group than in the controls. In addition, HIF2α, LDHA, and PFK1 levels tended to be higher. This is the first study on large animals showing an association between HIF, HIF target gene expression, and RIPC, and our findings suggest that HIF and its target genes may play a role in the RIPC phenomenon.

Despite recent studies showing neutral results [24, 25] regarding RIPC in CABG and STEMI patients, further studies are needed to fully understand the biological mechanisms behind RIPC. Promising results have been seen in pediatric studies [26]. The studies regarding adult populations have several comorbidities, and medications that might mask or dilute the protection offered by RIPC. A number of these factors including diabetes, age, and the use of certain medications, such as propofol or ticagrelor, have been identified [27, 28].

We acknowledge the small size as a limitation of this study. However, in our study histological, physiological, and biochemical means were simultaneously used to explore the effects of RIPC on cardiac function. All methods used in this study have been previously validated, and biochemical markers and echocardiography are clinically used also in humans [29, 30]. In invasive experiments in this animal model of juvenile piglets, the myocardiums of the studied animals were most likely normally perfused before the experiments, making standardized comparisons possible between the studied groups, while in human clinical studies formation of truly comparable groups is difficult even with randomization.

Recent clinical trials in adult human populations, albeit with very diseased patients, show contradictory results regarding the efficacy of RIPC [24, 31, 32]. However, widespread animal studies, including ours, indicate that RIPC would be beneficial.

In this study, the temperature of the animals was maintained at normothermia, but new studies have shown that the cardioprotective effect of RIPC has been improved when applied to the (40 °C) warmed limb. Warm-RIPC would be interesting to test in clinical settings [33].

Future studies should be conducted to further expand the molecular level understanding of the mechanisms and possible synergies behind the phenomenon. A detailed understanding of the molecular mechanisms behind RIPC will enable targeting them to improve cardioprotection. Our study backs up the implication that HIF and its glycolytic and vascular target genes play a part in this.

In conclusion, RIPC significantly reduced the infarct size in our large animal model, and it was also associated with lower levels of cardiac biomarkers and greater ventricular ejection fractions, emphasizing histolic and physiologic preservation of cardiac function after an acute myocardial infarction. HIF stabilization detected in the hind limbs and higher mRNA levels of the HIF targets GLUT1, GLUT4, GAPDH, ENO1, and eNOS in following

RIPC suggests an involvement of RIPC in cardiac protection.

Acknowledgements

The authors thank Seija Seljänperä, RN, for her help in caring for the animals and Tanja Aatsinki, biomedical laboratory scientist, for molecular analyses.

Disclosure statement

No potential conflict of interest was reported by the author(s).

Funding

This work was supported by The Finnish Foundation for Cardiovascular Research (Vesa Anttila), The Sigrid Jusélius Foundation, The Emil Aaltonen Foundation, and The Jane and Aatos Erkko Foundation (Peppi Koivunen).

References

[1] Tsao CW, Aday AW, Almarzooq ZI, et al. Heart disease and stroke statistics—2023 update: a report from the America Heart Association. Circulation. 2023;147(8):e93–e621. doi: 10.1161/CIR.0000000000001123.

[2] Walsh SR, Tang T, Sadat U, et al. Cardioprotection by remote ischaemic preconditioning. Br J Anaesth. 2007;99(5):611–616. doi: 10.1093/bja/aem273.

[3] Thielmann M, Kottenberg E, Kleinbongard P, et al. Cardioprotective and prognostic effects of remote ischaemic preconditioning in patients undergoing coronary artery bypass surgery: a single-centre randomised, double-blind, controlled trial. Lancet. 2013;382(9892):597–604. doi: 10.1016/S0140-6736(13)61450-6.

[4] Cheung MMH, Kharbanda RK, Konstantinov IE, et al. Randomized controlled trial of the effects of remote ischemic preconditioning on children undergoing cardiac surgery: first clinical application in humans. J Am Coll Cardiol. 2006;47(11):2277–2282. doi: 10.1016/j.jacc.2006.01.066.

[5] Lee SH, Wolf PL, Escudero R, et al. Early expression of angiogenesis factors in acute myocardial ischemia and infarction. N Engl J Med. 2000;342(9):626–633. doi: 10.1056/NEJM200003023420904.

[6] Cho YJ, Lee E, Lee K, et al. Long-term clinical outcomes of remote ischemic preconditioning and postconditioning outcome (RISPO) trial in patients undergoing cardiac surgery. Int J Cardiol. 2017;231:84–89. doi: 10.1016/j.ijcard.2016.12.146.

[7] Sardar P, Chatterjee S, Kundu A, et al. Remote ischemic preconditioning in patients undergoing cardiovascular surgery: evidence from a meta-analysis of randomized controlled trials. Int J Cardiol. 2016;221:34–41. doi: 10.1016/j.ijcard.2016.06.325.

[8] Kido M, Du L, Sullivan CC, et al. Hypoxia-inducible factor 1-alpha reduces infarction and attenuates progression of cardiac dysfunction after myocardial infarction in the mouse. J Am Coll Cardiol. 2005;46(11):2116–2124. doi: 10.1016/j.jacc.2005.08.045.

[9] Donato M, Bin EP, Annunzio VD, et al. Myocardial remote ischemic preconditioning: from cell biology to clinical application. Mol Cell Biochem. 2021;476(10):3857–3867. doi: 10.1007/s11010-021-04192-4.

[10] Bell SP, Sack MN, Patel A, et al. Delta opioid receptor stimulation mimics ischemic preconditioning in human heart muscle. J Am Coll Cardiol. 2000;36(7):2296–2302. doi: 10.1016/s0735-1097(00)01011-1.

[11] Belhomme D, Peynet J, Louzy M, et al. Evidence for preconditioning by isoflurane in coronary artery bypass graft surgery. Circulation. 1999;100(19 Suppl):II340–4. doi: 10.1161/01.cir.100.suppl_2.ii-340.

[12] Piot CA, Padmanaban D, Ursell PC, et al. Ischemic preconditioning decreases apoptosis in rat hearts *in vivo*. Circulation. 1997;96(5):1598–1604. doi: 10.1161/01.cir.96.5.1598.

[13] Kloner RA, Jennings RB. Consequences of brief ischemia: stunning, preconditioning, and their clinical implications: part 2. Circulation. 2001;104(25):3158–3167. doi: 10.1161/hc5001.100039.

[14] Yang J, Liu C, Du X, et al. Hypoxia inducible factor 1alpha plays a key role in remote ischemic preconditioning Against stroke by modulating inflammatory responses in rats. J Am Heart Assoc. 2018;7(5):e7589-94. doi: 10.1161/JAHA.117.007589.

[15] Albrecht M, Zitta K, Bein B, et al. Remote ischemic preconditioning regulates HIF-1alpha levels, apoptosis and inflammation in heart tissue of cardiosurgical patients: a pilot experimental study. Basic Res Cardiol. 2013;108(1):314–310. doi: 10.1007/s00395-012-0314-0.

[16] Cai Z, Luo W, Zhan H, et al. Hypoxia-inducible factor-1 is required for remote ischemic preconditioning of the heart. Proc Natl Acad Sci USA. 2013;110(43):17462–17467. doi: 10.1073/pnas.1317158110.

[17] Konstantinov IE, Li J, Cheung MM, et al. Remote ischemic preconditioning of the recipient reduces myocardial ischemia-reperfusion injury of the denervated donor heart via a katp channel-dependent mechanism. Transplantation. 2005;79(12):1691–1695. doi: 10.1097/01.tp.0000159137.76400.5d.

[18] Basalay MV, Mastitskaya S, Mrochek A, et al. Glucagon-like peptide-1 (GLP-1) mediates cardioprotection by remote ischaemic conditioning. Cardiovasc Res. 2016;112(3):669–676. doi: 10.1093/cvr/cvw216.

[19] Chao de la Barca JM, Bakhta O, Kalakech H, et al. Metabolic signature of remote ischemic preconditioning involving a cocktail of amino acids and biogenic amines. J Am Heart Assoc. 2016;5(9):e3891-3902. doi: 10.1161/JAHA.116.003891.

[20] Oba T, Yasukawa H, Nagata T, et al. Renal nerve-mediated erythropoietin release confers cardioprotection during remote ischemic preconditioning. Circ J. 2015;79(7):1557–1567. doi: 10.1253/circj.CJ-14-1171.

[21] Comita S, Rubeo C, Giordano M, et al. Pathways for cardioprotection in perspective: focus on remote conditioning and extracellular vesicles. Biology. 2023;12(2):308. doi: 10.3390/biology12020308.

[22] Chen H, Jing XY, Shen YJ, et al. Stat5-dependent cardioprotection in late remote ischaemia preconditioning. Cardiovasc Res. 2018;114(5):679–689. doi: 10.1093/cvr/cvy014.

[23] Semenza GL. Signal transduction to hypoxia-inducible factor 1. Biochem Pharmacol. 2002;64(5–6):993–998. doi: 10.1016/s0006-2952(02)01168-1.

[24] Hausenloy DJ, Candilio L, Evans R, et al. Remote ischemic preconditioning and outcomes of cardiac surgery. N Engl J Med. 2015;373(15):1408–1417. doi: 10.1056/NEJMoa1413534.

[25] Meybohm P, Bein B, Brosteanu O, et al. A multicenter trial of remote ischemic preconditioning for heart surgery. N Engl J Med. 2015;373(15):1397–1407. doi: 10.1056/NEJMoa1413579.

[26] Zhou W, Zeng D, Chen R, et al. Limb ischemic preconditioning reduces heart and lung injury after an open heart operation in infants. Pediatr Cardiol. 2010;31:22–29.

[27] Kottenberg E, Musiolik J, Thielmann M, et al. Interference of propofol with signal transducer and activator of transcription 5 activation and cardioprotection by remote ischemic preconditioning during coronary artery bypass grafting. J Thorac Cardiovasc Surg. 2014;147(1):376–382. doi: 10.1016/j.jtcvs.2013.01.005.

[28] Ferdinandy P, Hausenloy DJ, Heusch G, et al. Interaction of risk factors, comorbidities, and comedications with ischemia/reperfusion injury and cardioprotection by preconditioning, postconditioning, and remote conditioning. Pharmacol Rev. 2014;66(4):1142–1174. doi: 10.1124/pr.113.008300.

[29] Daubert MA, Jeremias A. The utility of troponin measurement to detect myocardial infarction: review of the current findings. Vasc Health Risk Manag. 2010;6:691–699. doi: 10.2147/vhrm.s5306.

[30] Joffe SW, Chalian A, Tighe DA, et al. Trends in the use of echocardiography and left ventriculography to assess left ventricular ejection fraction in patients hospitalized with acute myocardial infarction. Am Heart J. 2009;158(2):185–192. doi: 10.1016/j.ahj.2009.05.027.

[31] Sloth AD, Schmidt MR, Munk K, et al. Improved long-term clinical outcomes in patients with ST-elevation myocardial infarction undergoing remote ischaemic conditioning as an adjunct to primary percutaneous coronary intervention. Eur Heart J. 2014;35(3):168–175. doi: 10.1093/eurheartj/eht369.

[32] Pryds K, Terkelsen CJ, Sloth AD, et al. Remote ischaemic conditioning and healthcare system delay in patients with ST-segment elevation myocardial infarction. Heart. 2016;102(13):1023–1028. doi: 10.1136/heartjnl-2015-308980.

[33] Penna C, Sorge M, Tullio F, et al. A TRICK to improve the effectiveness of RIC: role of limb temperature in enhancing the effectiveness of remote ischemic conditioning. Biology. 2022;11(1):146. doi: 10.3390/biology11010146.